

Article

Not peer-reviewed version

Performance Enhancement of MRAC via Generalized Dynamic Inversion

[Alharith Mahmoud Fadlalah](#) * and [Abdulrahman Bajodah](#)

Posted Date: 18 July 2024

doi: 10.20944/preprints2024071513.v1

Keywords: Null control vector; Projection matrix; Model Reference Adaptive Control; Generalized Dynamic Inversion; Lyapunov Stability



Preprints.org is a free multidiscipline platform providing preprint service that is dedicated to making early versions of research outputs permanently available and citable. Preprints posted at Preprints.org appear in Web of Science, Crossref, Google Scholar, Scilit, Europe PMC.

Copyright: This is an open access article distributed under the Creative Commons Attribution License which permits unrestricted use, distribution, and reproduction in any medium, provided the original work is properly cited.

Article

Performance Enhancement of MRAC Via Generalized Dynamic Inversion

Alharith Mahmoud Fadlalah * and Abdulrahman H. Bajodah

King Abdulaziz University, Aeronautical Engineering Department, Jeddah, 21589 KSA; abajodah@kau.edu.sa

* Correspondence: hariethmahmoud@gmail.com

Abstract: Whilst Model Reference Adaptive Control theory provides mathematical techniques for achieving the performance of the system without undue dependence upon dynamic systems models, its applicability may not be suitable for systems that are crucial to safety due to suboptimal transient and error convergence performance. In this article, our approach enhances the performance of MRAC by utilizing a Generalized Dynamic Inversion (GDI). Two control actions are permitted under the GDI control law. One control is the particular part that is responsible for enforcing the reference system-constrained behaviors. Another control action is carried out by the control law's auxiliary component and is incorporated into the standard MRAC control law. This augmented part is referred to as a null control vector, and it is used to enhance the performance of MRAC. The classic MRAC control law, when supplemented with a null vector term consisting of an adaptive gain that changes in response to tracking errors, forces the dynamical system to behave similarly to the reference model. This null vector, in particular, restricts the oscillation intensity of the tracking errors, which is employed to generate the adaptive parameters. It is demonstrated that this critical element of our approach enhances transient performance and ensures that error dynamics vanish asymptotically. Extensive simulations have been conducted to prove the efficacy of the proposed method.

Keywords: null control vector; projection matrix; model reference adaptive control; generalized dynamic inversion; Lyapunov stability

1. Introduction

MRAC aims to ensure that the dynamical system emulates the prescribed behavior of a reference model. MRAC is a well-researched issue in the field of adaptive control. Even though the issue dates back to the 1950s, there are still many unresolved difficulties, most notably in the area of performance. There are two established methods for resolving the MRAC issue: direct MRAC as well as indirect MRAC [1–3]. The direct method updates the control parameters directly using a differential law, while the indirect approach updates the plant parameters differentially and then algebraically as a function of the plant identifying. To combine the advantages of both methodologies, researchers in [4] developed a combined MRAC strategy and proven its efficacy in a variety of applications. Simultaneously, scientists in [5] suggested a hybrid adaptive control framework for robotic systems, in which the adaptive parameters are based on both tracking and prediction errors. The combination/composite of these adaptive laws leads to a substantial improvement in transient performance. Furthermore, authors in [6–8] have made significant contributions to combined/composite structure.

The stability of the closed-loop system and the asymptotical convergence of the error dynamics to zero are guaranteed by the standard and combination techniques to MRAC without restricting the external reference input in any way. Therefore, unless the regressor signals meet rigorous criteria of persistent excitation can the parameter estimates be ensured to be accurate [1]. In [9], the authors demonstrated that the persistent excitation constraint on the regressor results in the reference input possessing the same number of spectral lines as the unknown parameters, though - the condition usually occurs to be quite limiting. Imposing the PE criterion via the external reference input may not always be feasible, and it is frequently impossible to monitor a signal's PE status online, even as criteria are dependent on the signal's predicted values. As a result, finding a realistic solution to

the parameter converging and transient response enhancement problems has been a lengthy research objective within adaptive control [10–16].

Numerous such efforts have been made in recent years to build adaptive methods for an enhanced transient response. Consolidated direct and indirect adaptation has been demonstrated to be capable, with simulations demonstrating milder transients when compared to either indirect or direct learning on their own [17–19]. While these papers established the stability of these mixed techniques, no firm guarantees of optimum transient response have been made, and this remains a theoretical possibility [20].

Another technique for interpreting the transient response is to employ a prescribed performance function that specifies the peak overshoot, error dynamics, and converging rate that were previously integrated into the adaptive control design [21]. Regrettably, the initial conditions must have been well acknowledged, and the error dynamics do not appear to be diminishing [22].

The Luenberger observer-based adaptive control technique can be utilized to enhance MRAC transient responsiveness by introducing an error feedback component to the reference model [23,24]. This strategy provides clear insight on transitory performance by boosting the rate of convergence of the error signal, but it does so by replacing the well-designed reference model, altering the intended output of the reference to be followed. Numerous authors in [25,26] attempt to improve the identification method by incorporating a high-order parameter estimator, that leads to dynamic certainty equivalency in a closed-loop adaptive system, hence improving transient response without relying on direct error normalizing.

The literature reviewed in this paper summarizes the problems that face the performance of the adaptive system and suggests numerous remedies, some of which are costly to adopt. As a result, research is being conducted in this area to improve MRAC's performance, particularly the asymptotic convergence of tracking errors and transient response. Therefore, In this paper, we propose an MRAC structure for dynamic systems stabilization and command follow-up that guarantees tracking error diminishes asymptotically and improves transient performance. Our method improves the performance of MRAC that is based on GDI. The GDI control method was already demonstrated to be efficient for spaceship controlling [27,28], particularly underactuated spaceflight [29], as well as robots manipulators [30]. Within the architecture of GDI, the Greville formula provides for two basic collaborating controllers: one which imposes the required constraints and another which enables an extra degree of design flexibility. This additional level of flexibility enables the incorporation of several design techniques inside GDI. The usage of a null projection matrix ensures that the auxiliary component operates on the constraint matrix's null space, whereas the particular part operates on the range space of the constraint matrix's transpose. The non-interference of control actions is ensured by the orthogonality of two control subspaces, and hence both actions strive forward into a single aim. Constraint dynamics incorporate the performance criteria and then are reversed using the Moore-Penrose generalized inverse to produce the reference system trajectories, i.e., the particular part is responsible for enforcing the reference system-constrained behaviors. Another control action is carried out by the control law's auxiliary component, which is carefully constructed and then implemented into the standard MRAC control law to improve MRAC performance.

2. Model Reference Adaptive Control Based Generalized Dynamic Inversion

The concept of employing GDI in adaptive control is introduced in this section.

2.1. GDI Control

To begin, we will provide a basic overview of GDI control. Two provisions comprise the GDI control law. The first type of controller is the particular controller, which imposes the specified constraints; the second type of controller is the auxiliary controller, which offers a degree of design freedom. This additional degree of freedom enables the incorporation of alternative design approaches within GDI. The usage of a null projection matrix ensures that the auxiliary controller operates on

the constraint matrix's nullspace, while the particular controller operates on the range space of the constraint matrix's transpose. The orthogonality of two control subspaces assures that control actions do not interfere with one another, ensuring that both actions operate toward a same objective. The following Figure 1 illustrates this description of GDI, where $\alpha^+\mu$ denotes the particular component, P is the null projection matrix, and Y denotes the null control vector, which should be carefully specified.

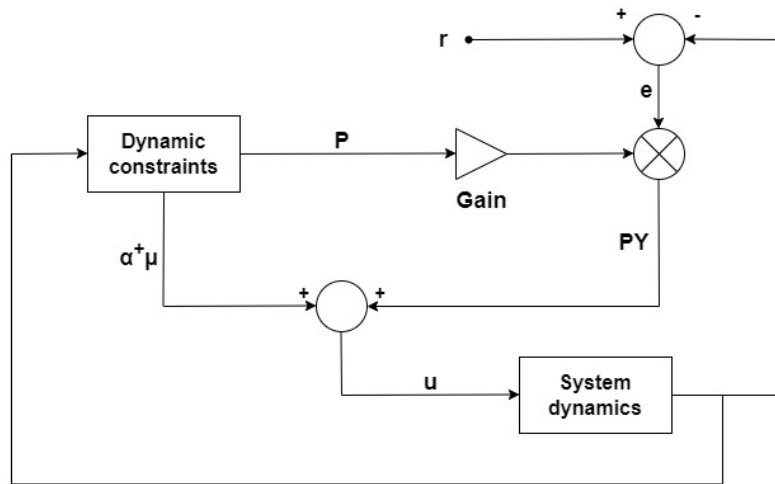


Figure 1. Block diagram of Generalized Dynamic Inversion control.

2.2. Reference Model

The reference model simulates the required closed loop dynamical system performance and its output is compared to the dynamical system's output. A system error signal is generated as a result of this comparison, which drives the online update of the law. For the purpose of enforcing constraints into reference model so that it can be followed, a reference model is constructed based on a particular component of the GDI control.

Assume the initial control target is to force a state variable $x_{s_j} \in x$ to track a scalar piecewise continuous function $r(t)$ asymptotically. A Virtual Constraint Dynamics (VCD) in x_{s_j} is first prescribed using the following LTI form.

$$c_{1,0}x_{s_j}^{(d_1)} + c_{1,1}x_{s_j}^{(d_1-1)} + \dots + c_{1,d_1-1}\dot{x}_{s_j} + c_{1,d_1}x_{s_j} = c_{1,d_1}r(t) \quad (1)$$

Where $r(t) \in L_\infty$ denotes the reference model's desired input, d_1 denotes the degree to which x_{s_j} is related to control vector u . For asymptotically stable results, we used $c_{1,0}, \dots, c_{1,d_1}$ as a positive real scalar constant.

Consider the following state space model for the linear time invariant (LTI) dynamical control system

$$\dot{x} = Ax + Bu \quad (2)$$

The state variable x_{s_j} and its first d_1 time derivative are defined as follows along the solution trajectories of (2).

$$x_{s_j}^{(i)} = I_{s_j} A^{(i)} x, i = 0, \dots, d_1 - 1, j = 1, 2, \dots, n \quad (3)$$

and

$$x_{s_j}^{(d_1)} = I_{s_j} (A^{d_1} x + A^{d_1-1} Bu) \quad (4)$$

Where I_{s_j} is the s_j^{th} of the identity matrix $I_{n \times n}$, and $A = I_{n \times n}$.

The differential form (1) of the VCD can now be expressed algebraically as follows.

$$\alpha_{s_j} u = \mu_{s_j} x + \gamma_{s_j}(t) \quad (5)$$

Where the control coefficients $\alpha_{s_j} \in \mathbb{R}^{1 \times m}$ is:

$$\alpha_{s_j} = c_{1,0} I_{s_j} A^{d_1-1} B \quad (6)$$

and $\mu_{s_j} x : \mathbb{R}^n \rightarrow \mathbb{R}$ and $\gamma_{s_j}(t) : \mathbb{R} \rightarrow \mathbb{R}$ are respectively the feedback and feedforward control load functions, where $\mu_{s_j} \in \mathbb{R}^{1 \times n}$ is:

$$\mu_{s_j} = - \sum_{i=0}^{d_1} c_{1,i} I_{s_j} A^{d_1-i} \quad (7)$$

and

$$\gamma_{s_j}(t) = c_{1,d_1} r(t) \quad (8)$$

Remark 2.1: In the case of an algebraic system (5) with $\alpha_{s_j} \neq 0_{1 \times m}$, a control vector u exists to implement the VCD (1) on system dynamics (2), rendering the algebraic system (5) consistent. Equation (4) shows that the criterion $\alpha_{s_j} \neq 0_{1 \times m}$ is satisfied by (2) because x_{s_j} has a clearly defined relative degree with regard to u , implying that (5) is consistent.

Equation (5) is an under-determined algebraic system with an infinite number of possible solutions. The Greville approach [31–33] provides the general solution, which results in

$$u = \underbrace{\alpha_{s_j}^+ (\mu_{s_j} x + \gamma_{s_j}(t))}_{\in R(\alpha_{s_j}^T)} + \underbrace{P_{s_j} y}_{\in N(\alpha_{s_j})} \quad (9)$$

Where $\alpha_{s_j}^+ \in \mathbb{R}^m$ is the MPGI of α_{s_j} , and is given by:

$$\alpha_{s_j}^+ = \frac{\alpha_{s_j}^T}{\alpha_{s_j} \alpha_{s_j}^T} \quad (10)$$

and $P_{s_j} \in \mathbb{R}^{m \times m}$ is the projection matrix on the nullspace of α_{s_j} and is given by:

$$P_{s_j} = I_{m \times m} - \alpha_{s_j}^+ \alpha_{s_j} \quad (11)$$

The reference model is expressed as an LTI model in the following:

$$\dot{x}_m = A_m x_m + B_m r(t) \quad (12)$$

Where $A_m \in \mathbb{R}^{n \times n}$ represents Hurwitz matrix, $r(t)$ is bounded input signal, and $x_m \in \mathbb{R}^n$ denotes reference model state.

The reference model is generated as follows by substituting a particular portion of (9) into (2) and comparing the results with (12).

$$A_m = A + B \alpha_{s_j}^+ \mu_{s_j} \quad (13)$$

$$B_m = c_{1,d_1} B \alpha_{s_j}^+ \quad (14)$$

Remark 2.2: Multiple constraint dynamics may be used in the event of insufficient stability. This phenomena is discussed in further detail later in this article with reference to three-axis coupling flying wing aircraft.

2.3. Design of an Adaptive Control System

We will begin by providing an overview of MRAC, followed by the proposed strategy for improving the performance of MRAC.

2.3.1. Classical MRAC

To begin, we will provide a brief overview of model-reference adaptive control. Consider the dynamical system denoted by

$$\dot{x} = Ax + B\Lambda u \quad (15)$$

Where $A \in \mathbb{R}^{n \times n}$ is the unknown system matrix, $x = [x_1 \dots x_n] \in \mathbb{R}^{n \times 1}$ is the accessible state vector, $B \in \mathbb{R}^{n \times m}$ is the nominal control matrix due to uncertainty in actuators, $u = [u_1 \dots u_m]^T \in \mathbb{R}^m$ is the control vector, and $\Lambda \in \mathbb{R}^{m \times m}$ is the actuator effectiveness matrix, which is a diagonal matrix $[\lambda_1, \lambda_2, \dots, \lambda_m]$ and it is unknown.

Within MRAC, a reference model (12) has been selected to reflect the system's desired closed-loop response of (15).

The adaptive control law is described as [34] consisting of a linear feedback component and a linear feedforward component.

$$u = K_x(t)x + K_r(t)r \quad (16)$$

There are two control gains that change over time: $K_x(t) \in \mathbb{R}^{n \times m}$ and $K_r(t) \in \mathbb{R}^{m \times m}$. These are called direct estimates of the control parameters.

Substituting (16) in (15) results in

$$\dot{x} = (A + B\Lambda K_x(t))x + B\Lambda K_r(t)r \quad (17)$$

To aid in the design purpose of making system (17) behave like the selected reference model of (12), the following matching conditions are presented [34,35].

Assumption 1. There are ideal matrices $K_x^* \in \mathbb{R}^{n \times m}$ and $K_r^* \in \mathbb{R}^{m \times m}$ that have the property that

$$A + B\Lambda K_x^* = A_m \quad (18)$$

$$B\Lambda K_r^* = B_m \quad (19)$$

Utilizing (18) and (19), the closed-loop system in (17) can be represented by the following equation

$$\dot{x} = A_m x + B_m r + B\Lambda \tilde{K}_x + B\Lambda \tilde{K}_r \quad (20)$$

Where $\tilde{K}_x \triangleq K_x(t) - K_x^*$ and $\tilde{K}_r(t) \triangleq K_r(t) - K_r^*$

The tracking error can be described as follows:

$$e(t) \triangleq x(t) - x_m(t) \quad (21)$$

Utilizing (12), (20) and (21), the obtained error dynamic is

$$\dot{e} = A_m e + B\Lambda \tilde{K}_x x + B\Lambda \tilde{K}_r r \quad (22)$$

The adaptive laws are obtained as [34]

$$\dot{K}_x^T = -\Gamma_x x e^T P B s g n \Lambda \quad (23)$$

$$\dot{K}_r^T = -\Gamma_r r e^T P B s g n \Lambda \quad (24)$$

Γ_x and Γ_r signify appropriate dimension positive-definite learning rate matrices. The positive-definite matrix $P \in \mathbb{R}^{n \times n}$ can be solved using the Lyapunov equation

$$A_m^T P + P A_m + Q = 0 \quad (25)$$

Where $Q \in \mathbb{R}^{n \times n}$ is any obtained positive-definite matrix.

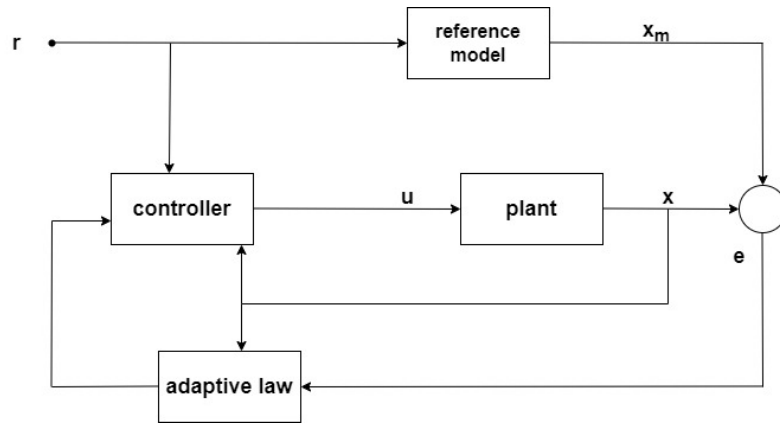


Figure 2. Model Reference Adaptive Control.

Remark 2.3: Despite the fact that equations (16), (23) and (24) ensure that the error between both the dynamical system in (15) and the reference model in (12) reduces asymptotically ($e(t) \rightarrow 0$ as $t \rightarrow \infty$), practically, the trajectory of the dynamical system can deviate significantly from the trajectory of the reference model during the learning stage (transient phase). This issue is known as the poor transient response problem.

Remark 2.4: The tracking error $e(t)$ is an essential part of MRAC. Because the update laws (23) and (24) are influenced by this error, the control law (16) may exhibit oscillations of its own if the error includes any elevated fluctuations.

Remark 2.5: As the dynamic system's complexity develops, it becomes more susceptible to parametric uncertainty. As a result, the typical MRAC system is incapable of providing a convenient performance. Specifically, MRAC cannot ensure that the error will converge to zero practically.

2.3.2. Modified MRAC

Motivating from the prior remarks on MRAC performance, our goal is to ensure that the tracking errors vanish asymptotically and to improve MRAC transient response. This will be accomplished by modifying the MRAC control law (16) to include the nullspace parameterization provided by the Greville formula in equation (9).

The following is a proposal for a null control vector ($y \in \mathbb{R}^m$) that is projected through a projection matrix ($P_n \in \mathbb{R}^{n \times n}$) to act on the control coefficient's nullspace and it is chosen to be a function of tracking error to speed up the error dynamics.

$$y = K_n(t)(x - x_m) = K_n(t)e \quad (26)$$

Where $K_n \in \mathbb{R}^{m \times n}$ is the gain of the null control vector and it will be adaptively generated using the Lyapunov candidate function.

Now, the control law for the modified MRAC can be written in the following form

$$u = \tilde{K}_x x + \tilde{K}_r r + P_n y \quad (27)$$

This implies the following:

$$u = \tilde{K}_x x + \tilde{K}_r r + P_n K_n(t) e \quad (28)$$

Remark 2.6: Despite the fact that the expression for P_n given by (11) contains the MPGI function α^+ , still maintains bounded due to the fact that it is a projection matrix function.

Now, by substituting (28) in (15), the following closed-loop system is obtained

$$\dot{x} = Ax + B\Lambda(\tilde{K}_x x + \tilde{K}_r r + P_n K_n(t) e) \quad (29)$$

or

$$\dot{x} = Ax + B\Lambda\tilde{K}_x x + B\Lambda\tilde{K}_r r + B\Lambda P_n K_n(t) e \quad (30)$$

Equation (28) must be enforce the tracking errors to dissipate asymptotically in such a way that

$$\lim_{t \rightarrow \infty} \|x(t) - x_m(t)\| = 0 \quad (31)$$

This implies that the error dynamics can be expressed as

$$\dot{e} = \dot{x} - \dot{x}_m \quad (32)$$

By utilizing the matching conditions in **Assumption 1.** and substituting (30) and (12) in equation (32), the error dynamics of the modified MRAC is obtained as follows

$$\dot{e} = A_m e + B\Lambda\tilde{K}_x x + B\Lambda\tilde{K}_r r + B\Lambda P_n K_n(t) e \quad (33)$$

Remark 2.7: According to the description of the error dynamics (33), the projected null control vector on the nullspace of control coefficients is composed of a gain that is adaptively adjusted in response to the tracking error, which plainly effects the system error. The update law is prevented from learning from the oscillations content of the system error in this manner.

The following is Lyapunov candidate function that we will use to derive the adaptive parameters.

$$V(e, \tilde{K}_x, \tilde{K}_r, K_n) = e^T P e + \text{trace}(|\Lambda| \tilde{K}_x \Gamma_x^{-1} \tilde{K}_x^T) + \text{trace}(|\Lambda| \tilde{K}_r \Gamma_r^{-1} \tilde{K}_r^T) + \text{trace}(|\Lambda| K_n \Gamma_n^{-1} K_n^T) \quad (34)$$

Now, the derivative of Lyapunov function is obtained as:

$$\begin{aligned} \dot{V}(e, \tilde{K}_x, \tilde{K}_r, K_n) = & e^T P \dot{e} + \dot{e}^T P e + \text{trace}(|\Lambda| \dot{\tilde{K}}_x \Gamma_x^{-1} \tilde{K}_x^T) + \text{trace}(|\Lambda| \tilde{K}_x \Gamma_x^{-1} \dot{\tilde{K}}_x^T) + \\ & \text{trace}(|\Lambda| \dot{\tilde{K}}_r \Gamma_r^{-1} \tilde{K}_r^T) + \text{trace}(|\Lambda| \tilde{K}_r \Gamma_r^{-1} \dot{\tilde{K}}_r^T) + \\ & \text{trace}(|\Lambda| \dot{K}_n \Gamma_n^{-1} K_n^T) + \text{trace}(|\Lambda| K_n \Gamma_n^{-1} \dot{K}_n^T) \end{aligned} \quad (35)$$

By using the properties of trace, equation (35) can be formulated as

$$\begin{aligned} \dot{V}(e, \tilde{K}_x, \tilde{K}_r, K_n) = & 2e^T P \dot{e} + 2\text{trace}(|\Lambda| \dot{\tilde{K}}_x \Gamma_x^{-1} \tilde{K}_x^T) + \\ & 2\text{trace}(|\Lambda| \dot{\tilde{K}}_r \Gamma_r^{-1} \tilde{K}_r^T) + 2\text{trace}(|\Lambda| \dot{K}_n \Gamma_n^{-1} K_n^T) \end{aligned} \quad (36)$$

Now, by using (33), equation (36) can be formulated as

$$\begin{aligned}\dot{V}(e, \tilde{K}_x, \tilde{K}_r, K_n) = & (e^T P A_m e + e^T A_m^T P e) \\ & + \underbrace{2e^T P B \Lambda \tilde{K}_x x}_{1 \times 1} + \underbrace{2e^T P B \Lambda \tilde{K}_r r}_{1 \times 1} + \\ & \underbrace{2e^T P B \Lambda P_n K_n e}_{1 \times 1} + 2\text{trace}(|\Lambda| \tilde{K}_x \Gamma_x^{-1} \dot{\tilde{K}}_x^T) + \\ & 2\text{trace}(|\Lambda| \tilde{K}_r \Gamma_r^{-1} \dot{\tilde{K}}_r^T) + 2\text{trace}(|\Lambda| K_n \Gamma_n^{-1} \dot{K}_n^T)\end{aligned}\quad (37)$$

Using (25) and then the following relations

$$e^T P B \Lambda \tilde{K}_x x = \text{trace}(|\Lambda| \tilde{K}_x x e^T P B \text{sgn} \Lambda) \quad (38)$$

$$e^T P B \Lambda P_n K_n e = \text{trace}(|\Lambda| K_n e e^T P B P_n \text{sgn} \Lambda) \quad (39)$$

$$e^T P B \Lambda \tilde{K}_r r = \text{trace}(|\Lambda| \tilde{K}_r r e^T P B \text{sgn} \Lambda) \quad (40)$$

Then,

$$\begin{aligned}\dot{V}(e, \tilde{K}_x, \tilde{K}_r, K_n) = & -e^T Q e + 2\text{trace}[|\Lambda| \tilde{K}_x (x e^T P B \text{sgn} \Lambda + \Gamma_x^{-1} \dot{\tilde{K}}_x^T)] + \\ & 2\text{trace}[|\Lambda| \tilde{K}_r (r e^T P B \text{sgn} \Lambda + \Gamma_r^{-1} \dot{\tilde{K}}_r^T)] + \\ & 2\text{trace}[|\Lambda| K_n (e e^T P B P_n \text{sgn} \Lambda + \Gamma_n^{-1} \dot{K}_n^T)]\end{aligned}\quad (41)$$

Now the adaptive parameters can be constructed as

$$\dot{\tilde{K}}_x^T = -\Gamma_x x e^T P B \text{sgn} \Lambda \quad (42)$$

$$\dot{K}_n^T = -\Gamma_n e e^T P B P_n \text{sgn} \Lambda \quad (43)$$

$$\dot{\tilde{K}}_r^T = -\Gamma_r r e^T P B \text{sgn} \Lambda \quad (44)$$

Theorem 1. Considering the dynamical system obtained by equation (15), the reference model denoted by equation (12), and the control law obtained by equation (28), with accordance to equations (42), (43), and (44). Hence, the trajectory provided by equation (33) ensured that the tracking errors vanish asymptotically.

Proof of Theorem 1. Based on equations (42), (43), and (44), equation (41) will follow that

$$\dot{V}(e, \tilde{K}_x, \tilde{K}_r, K_n) = -e^T Q e \leq -\lambda_{\min}(Q) \|e\|_2^2 \leq 0 \quad (45)$$

Equation (45) will result in $e(t)$, $K_n(t)$, $\tilde{K}_r(t)$, and $\tilde{K}_x(t)$ are really bounded and hence

$$\lim_{t \rightarrow \infty} V(e, \tilde{K}_x, \tilde{K}_r, K_n) = V(e_0, K_{n_0}, \tilde{K}_{r_0}, \tilde{K}_{x_0}) - \lambda_{\min}(Q) \|e\|_2^2 \quad (46)$$

Now by checking the derivative of $\dot{V}(e, \tilde{K}_x, \tilde{K}_r, K_n)$, we can prove that it is uniformly continuous.

$$\ddot{V}(e, \tilde{K}_x, \tilde{K}_r, K_n) = -\dot{e}^T Q e - e^T Q \dot{e} \quad (47)$$

$$\ddot{V}(e, \tilde{K}_x, \tilde{K}_r, K_n) = -2e^T Q (A_m e - B \Lambda \tilde{K}_x x - B \Lambda \tilde{K}_r r - B \Lambda K_n e) \quad (48)$$

Because $K_n(t)$, $e(t)$, $K_x(t)$, $K_r(t)$ are bounded by the fact that $\dot{V}(e, \tilde{K}_x, \tilde{K}_r, K_n) \leq 0$, the trajectories $x(t)$ is bounded due to $x_m(t)$ and $e(t)$ are bounded, reference signal $r(t)$ is also bounded, hence, $\dot{V}(e, \tilde{K}_x, \tilde{K}_r, K_n)$ is obviously uniformly continuous. This explain that $\dot{V}(e, \tilde{K}_x, \tilde{K}_r, K_n) \rightarrow 0$, and $e(t) \rightarrow 0$ as $t \rightarrow \infty$, and hence the error dynamics achieve asymptotic stability. \square

Remark 2.8: Theorem 1 emphasizes stability and good performance during both the transient and steady-state periods. Clearly $\lim_{t \rightarrow \infty} (x(t) - x_m(t)) = 0$, implying that the state trajectories $x(t)$ asymptotically approaches the reference model $x_m(t)$ of equation (12). Additionally, the control law (28) generated based on the null control vector (27) projected by a projection matrix (11) to act on the null space of control coefficients, or in other words, it forces the dynamical system (15) to behave similarly to the reference model throughout the system's response.

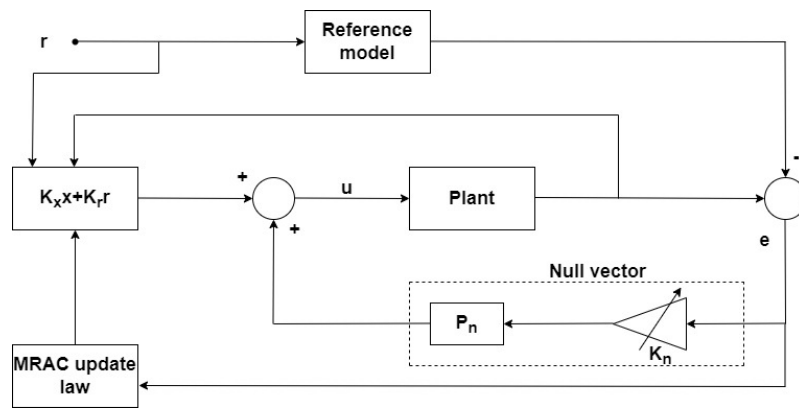


Figure 3. Modified Model Reference Adaptive Control.

3. Application to Aircraft Longitudinal and Lateral-Directional Control

Considering flying wing aircraft as an example, this section describes how the proposed method can be implemented.

3.1. Aircraft Dynamic Model

Figure 4 depicts an illustration of flying wing aircraft. It features two sets of elevons and split drag rudders. The inboard elevons are mostly used to regulate pitch; and positive deflection is considered as symmetric downward deflection; The outboard elevons are employed to control the roll of the vehicle through differential deflection. Yaw control is handled by split drag rudders.

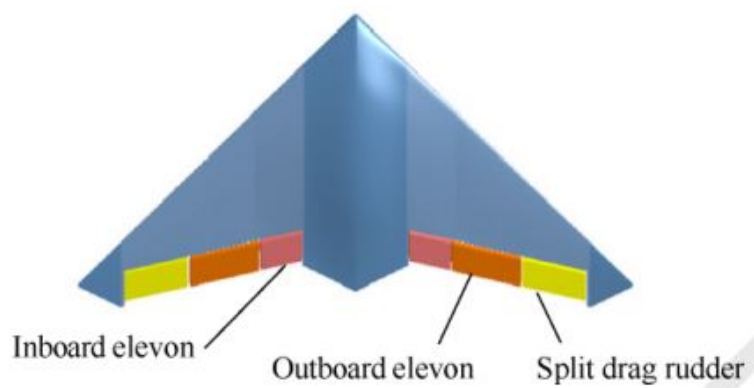


Figure 4. Flying Wing Aircraft.

Equations (49) and (50) as [36] depict the dynamic model in which the sideslip angle affects both the longitudinal and lateral dynamics, resulting in longitudinal and lateral-directional coupling. The instance aircraft's dynamic modes are listed in Table 1.

$$A = \begin{bmatrix} -0.96260 & -0.1736 & 0 & 1 & 0 \\ 0 & -0.0131 & 0.0301 & 0 & -0.9995 \\ 0 & -27.2058 & -12.9393 & 0 & -2.5551 \\ 35.9530 & 1.7764 & 0 & -5.2812 & 0 \\ 0 & -4.3583 & 1.9792 & 0 & -0.2942 \end{bmatrix} \quad (49)$$

$$B = \begin{bmatrix} 0 & -0.1911 & 0.0033 \\ 0 & 0 & 0.0024 \\ -136.1101 & 0 & -4.0272 \\ 0 & -116.9258 & 3.8804 \\ 0.9270 & 0 & -5.0404 \end{bmatrix} \quad (50)$$

Corresponding to the structure in fig 4, the angle of attack, sideslip angle, roll rate, pitch rate, and yaw rate have been chosen as accessible state variables for flying wing aircraft. The control variables are chosen to be δ_a , δ_e , and δ_r signifying inboard elevons (for roll), outboard elevons (for pitch), and drag rudders (for yaw).

$$x = [\alpha \quad \beta \quad p \quad q \quad r]^T \quad (51)$$

$$u = [\delta_a \quad \delta_e \quad \delta_r]^T \quad (52)$$

Table 1. Aircraft Dynamic Modes.

Mode	Eigen value
Short period	-9.4949
	3.2511
Dutch roll	-3.6965
	2.4777
Roll subsidence	-12.0279

3.2. Reference Model

As shown in Table 1, both short period and dutch roll are dynamically unstable, but the properties of roll mode are rather excellent. This means that the design of a reference model must concentrate on enhancing the aircraft's short-period and dutch-roll modes in order to attain stability and high performance. Therefore, the yaw-pitch axis will be subjected to the dynamic constraints.

3.2.1. First Constraint {r} Configuration

Put $x_{s_j} = r$ implies that $s_j = 5$ and $d_1 = d_{\{r\}} = 1$. Hence the values of $\alpha_{\{r\}}$, $\alpha_{\{r\}}^+$, and $P_{\{r\}}$ are obtained by equations (6), (10), and (11) as follows

$$\alpha_{\{r\}} = [0.9270 \quad 0 \quad -5.0404] \quad (53)$$

$$\alpha_{\{r\}}^+ = [0.0353 \quad 0 \quad -0.1919]^T \quad (54)$$

$$P_{\{r\}} = \begin{bmatrix} 0.9673 & 0 & 0.1779 \\ 0 & 1 & 0 \\ 0.1779 & 0 & 0.0327 \end{bmatrix} \quad (55)$$

The controller that enforce the constraint is obtained as

$$K_{\{r\}} = \alpha_{\{r\}}^+ \mu_{\{r\}} \quad (56)$$

$$K_{\{r\}} = \begin{bmatrix} 0 & 0.1538 & -0.0699 & 0 & -0.0426 \\ 0 & 0 & 0 & 0 & 0 \\ 0 & -0.8364 & 0.3798 & 0 & 0.2314 \end{bmatrix} \quad (57)$$

This implies that

$$A_m = \begin{bmatrix} -0.9626 & -0.1764 & 0.0013 & 1 & 0.0008 \\ 0 & -0.0151 & 0.0310 & 0 & -0.9989 \\ 0 & -44.7743 & -4.9610 & 0 & 2.3055 \\ 35.9530 & -1.4691 & 1.4739 & -5.2812 & 0.8979 \\ 0 & 0 & 0 & 0 & -1.5 \end{bmatrix} \quad (58)$$

Table 2 demonstrates the dynamical modes of the first constraint configuration. the table shows that the first constraint configuration stabilizes the dutch-roll mode, but short-period mode is still dynamically unstable.

Table 2. First constraint Dynamic Modes.

Mode	Eigen value
Short period	3.2511
	-9.4949
Dutch roll	-0.3139
	-1.5
Roll subsidence	-4.6623

3.2.2. Second Constarint {q} Configuration

The state and control matrices produced from the first constraint configuration are as follows

$$A_{\{r\}} = \begin{bmatrix} -0.9626 & -0.1764 & 0.0013 & 1 & 0.0008 \\ 0 & -0.0151 & 0.0310 & 0 & -0.9989 \\ 0 & -44.7743 & -4.9610 & 0 & 2.3055 \\ 35.9530 & -1.4691 & 1.4739 & -5.2812 & 0.8979 \\ 0 & 0 & 0 & 0 & -1.5 \end{bmatrix} \quad (59)$$

$$B_{\{r\}} = BP_{\{r\}} \quad (60)$$

$$B_{\{r\}} = \begin{bmatrix} 0.0006 & -0.1911 & 0.0001 \\ 0.0004 & 0 & 0.0001 \\ -132.3733 & 0 & -24.3453 \\ 0.6903 & -116.9258 & 0.1270 \\ 0 & 0 & 0 \end{bmatrix} \quad (61)$$

Now, put $x_{s_j} = q$ implies that $s_j = 4$ and $d_1 = d_{\{q\}} = 1$. Hence the values of $\alpha_{\{r,q\}}$, $\alpha_{\{r,q\}}^+$, and $P_{\{r,q\}}$ are obtained as

$$\alpha_{\{r,q\}} = \begin{bmatrix} 0.6903 & -116.9258 & 0.1270 \end{bmatrix} \quad (62)$$

$$\alpha_{\{r,q\}}^+ = \begin{bmatrix} 0.0001 & -0.0086 & 0 \end{bmatrix}^T \quad (63)$$

$$P_{\{r,q\}} = \begin{bmatrix} 1 & 0.0059 & 0 \\ 0.0059 & 0 & 0.0011 \\ 0 & 0.0011 & 1 \end{bmatrix} \quad (64)$$

The controller that enforce the second constraint is obtained as

$$K_{\{r,q\}} = \begin{bmatrix} -0.0018 & 0.0001 & 0.0003 & 0 & 0 \\ 0.3075 & -0.0126 & -0.0424 & 0.0009 & 0.0077 \\ -0.0003 & 0 & 0 & 0 & 0 \end{bmatrix} \quad (65)$$

Now, equations (13) and (14) implies that

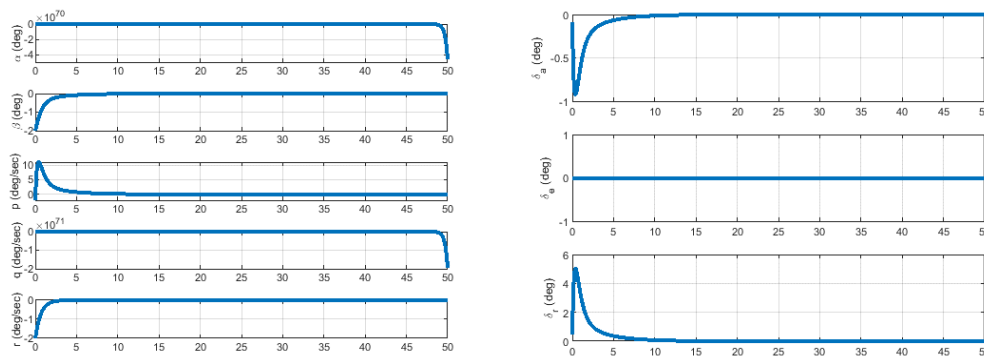
$$A_m = \begin{bmatrix} -1.0214 & -0.1740 & 0.0094 & 0.9998 & -0.0007 \\ 0 & -0.0151 & 0.0310 & 0 & -0.9989 \\ 0.2484 & -44.7845 & -4.9953 & 0.0007 & 2.3117 \\ 0 & 0 & 6.4349 & -5.3812 & 0 \\ 0 & 0 & 0 & 0 & -1.5 \end{bmatrix} \quad (66)$$

$$B_m = \begin{bmatrix} 0.0002 \\ 0 \\ -0.0007 \\ 0.1 \\ 0 \end{bmatrix} \quad (67)$$

Table 3 highlighted that the second constraint stabilized the modes of the aircraft i.e. A_m is Lyapunov stable.

Table 3. Second constraint Dynamic Modes.

Mode	Eigen value
Short period	-5.0931+0.53939i
	-5.0931-0.53939i
Dutch roll	-0.3485
	-1.5
Roll subsidence	-0.8783



(a) First constraint reference model

(b) First constraint control variables

Figure 5. Yaw rate constraint configuration.

3.3. Adaptive System Simulation

Simulated results are now provided to show the suggested method's superior performance over the traditional MRAC. The resulting findings were achieved using the MATLAB software, and the computer simulation used the Ode45 as a numerical solver. The reference model adopted is Figure 6, which constrains the yaw and pitch rates.

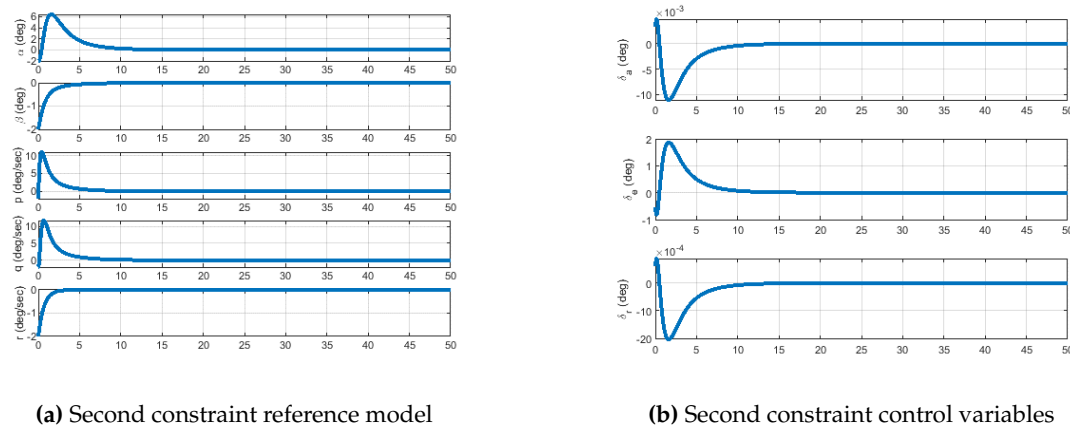


Figure 6. Yaw and pitch rates constraint configuration vs. t .

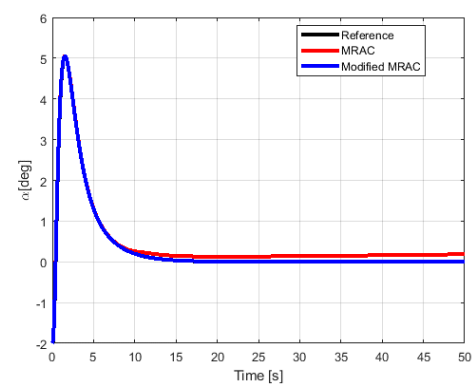
3.3.1. First Case Study

Figures 7–11 were created with learning rates of $\Gamma_x = 0.95$, $\Gamma_r = 10$, and $\Gamma_n = 100$.

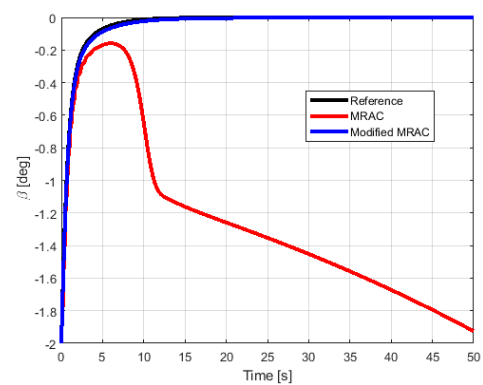
By examining Figure 7, it is obvious that the modified MRAC method achieves precise tracking of the reference model and produces smooth trajectories. As illustrated in Figure 7b, MRAC is unable to achieve acceptable tracking performance for sideslip angle due to a minor drift in the corresponding adaptive parameter. Additionally, as a result of the learning rate, figure 7e demonstrates oscillatory behavior. The suggested scheme overcomes these disadvantages by incorporating equation (26) into the control law of classic MRAC in order to address the tracking error problem. Furthermore, the projection matrix used in equation (11) permits the null control vector to act on the null space of control coefficients, suppressing the oscillations.

The error dynamics of both MRAC and modified MRAC are depicted in Figure 8. As illustrated in Figure 8a, the error dynamic does not totally converge to zero; additionally, it contains oscillations, which drive the adaptive parameters as seen in Figure 9. On the other hand, as illustrated in Figure 8b, the proposed method ensures that the error is convergent and free of fluctuations, corroborating theorem 2.1. The temporal history of adaptive parameters governed by modified MRAC error dynamics is depicted in Figure 10.

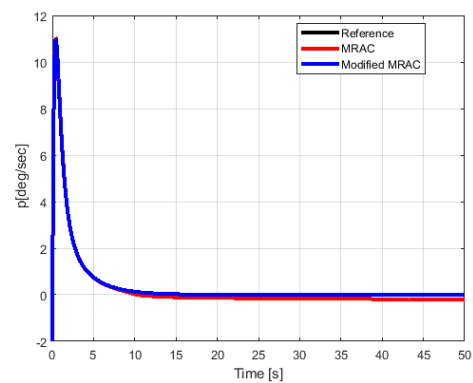
The control history of both methods is depicted in Figure 11. Our approach's control response is obviously superior to that of traditional MRAC. Additionally, as illustrated in Figure 11b, the suggested scheme's control is very similar to the control that forces the reference model to respect constraints (see Figure 6b), and hence equation (28) influences the adaptive system to behave similarly to the reference model.



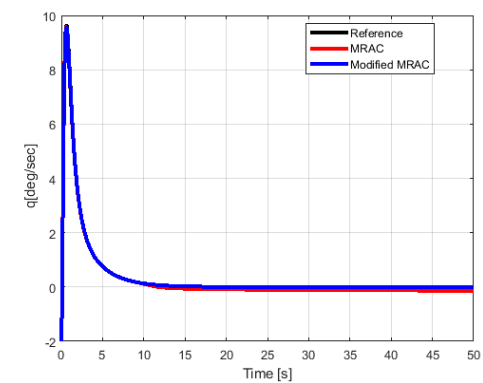
(a) Behavior of angle of attack



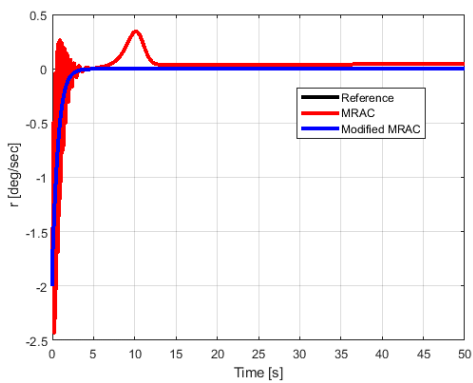
(b) Behavior of sideslip angle



(c) Behavior of roll angle rate

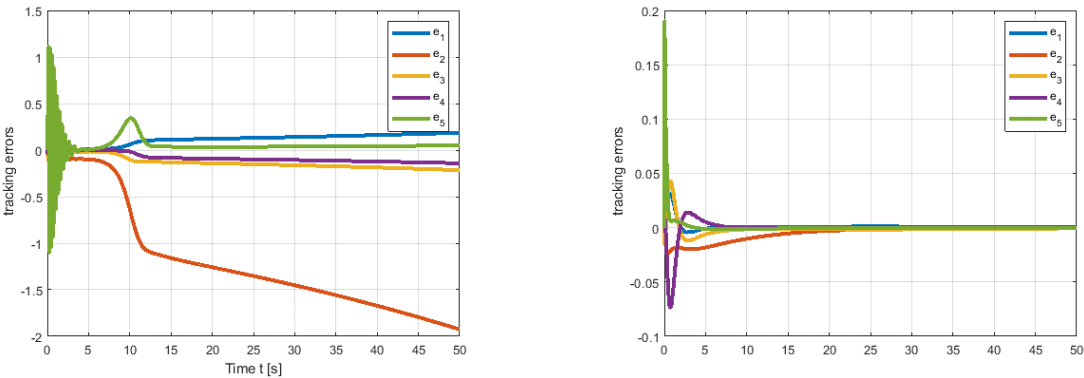


(d) Behavior of pitch angle rate

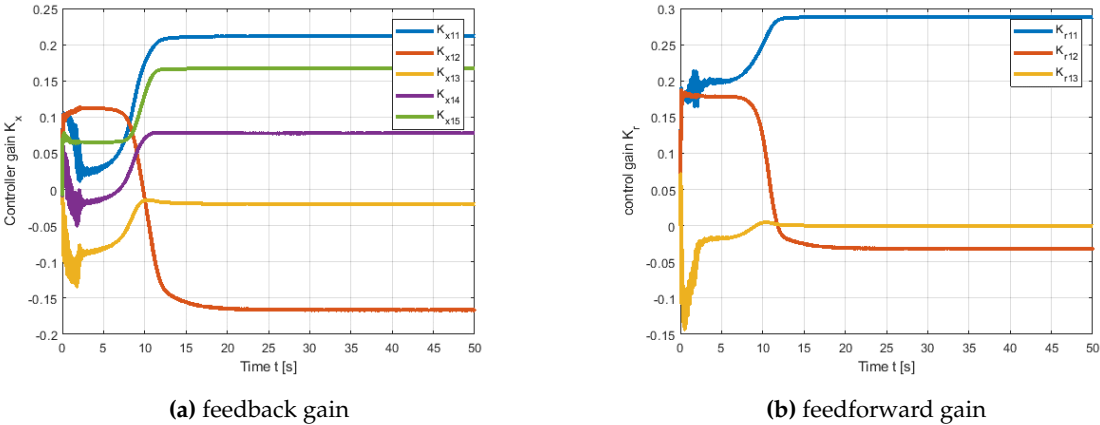


(e) Behavior of yaw angle rate

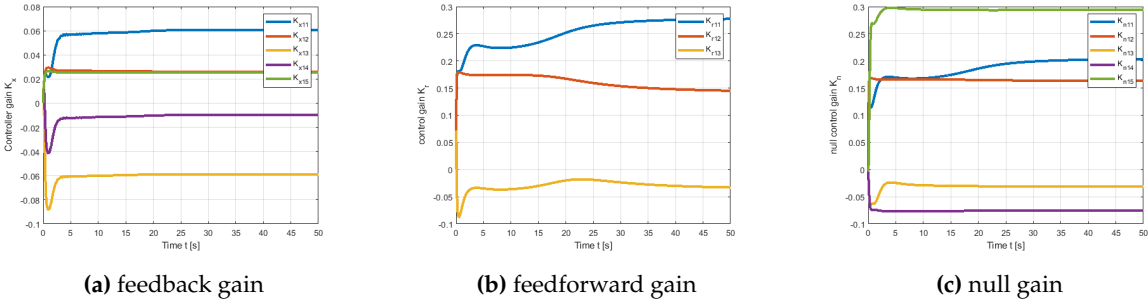
Figure 7. System states with Reference, MRAC, and Modified MRAC.



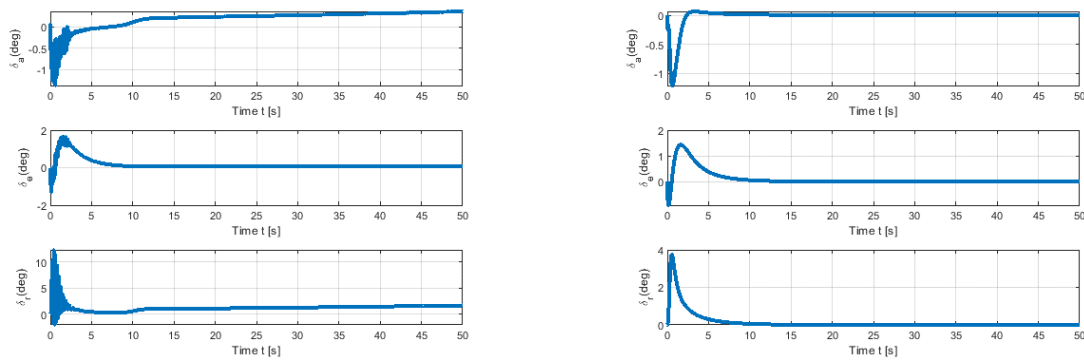
(a) MRAC tracking errors (b) Modified MRAC tracking errors vs.t.
Figure 8. Error dynamics with MRAC and modified MRAC.



(a) feedback gain (b) feedforward gain
Figure 9. MRAC adaptive parameters.



(a) feedback gain (b) feedforward gain (c) null gain
Figure 10. Modified MRAC adaptive parameters.



(a) MRAC control variables

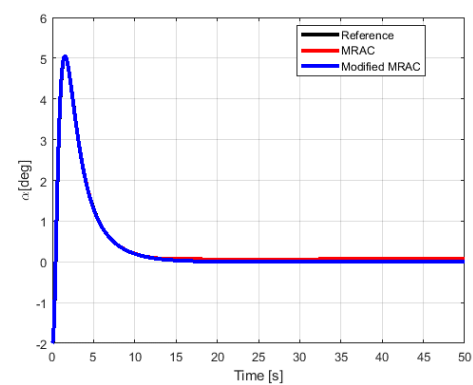
(b) Modified MRAC control variables

Figure 11. MRAC and modified MRAC control commands.

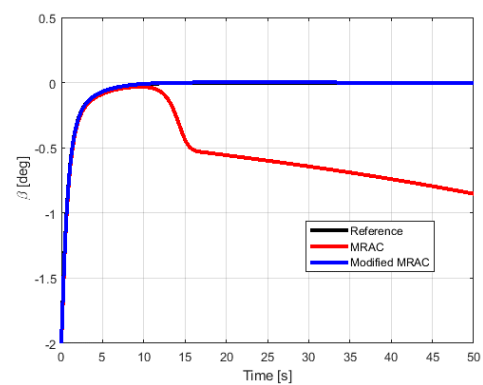
3.3.2. Second Case Study

Figures 12–fig:16 have been generated with tuning gains of $\Gamma_x = 10$, $\Gamma_r = 15$, and $\Gamma_n = 500$. Here, we would like to emphasize that the structure of the proposed scheme clearly limits adaptive parameter oscillations (as illustrated in Figure 15) and results in a reduction control input oscillations (as illustrated in figure 16b), and thus the error dynamics of the modified MRAC (as illustrated in figure 13b) do not encapsulate any of these oscillations.

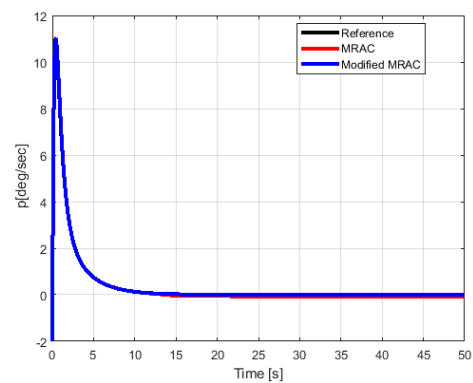
Since adaptive parameters and control inputs have minimized oscillations, the trajectory of the states for the modified MRAC scheme will have to be smooth, as illustrated in Figure 12.



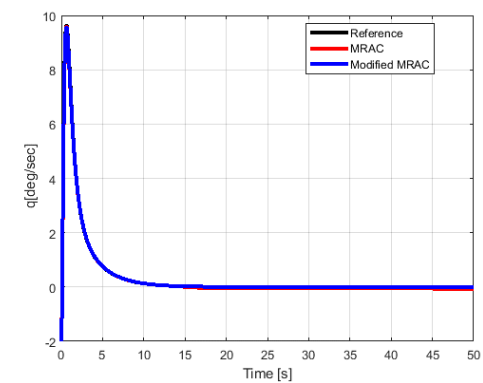
(a) Behavior of angle of attack



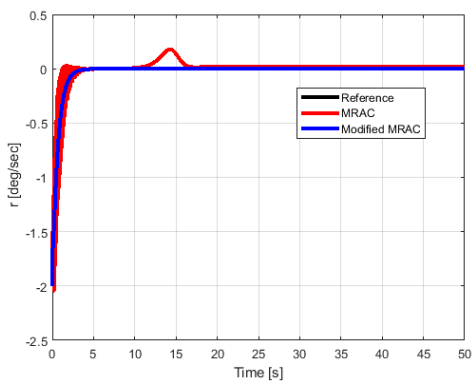
(b) Behavior of sideslip angle



(c) Behavior of roll angle rate

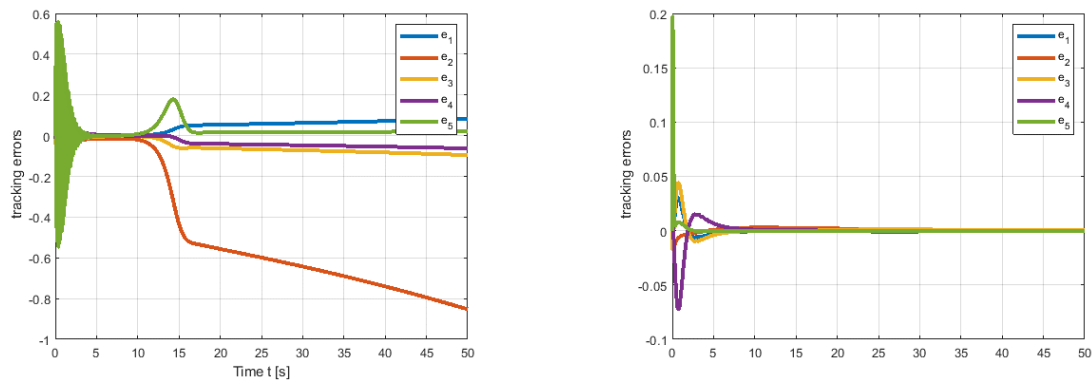


(d) Behavior of pitch angle rate

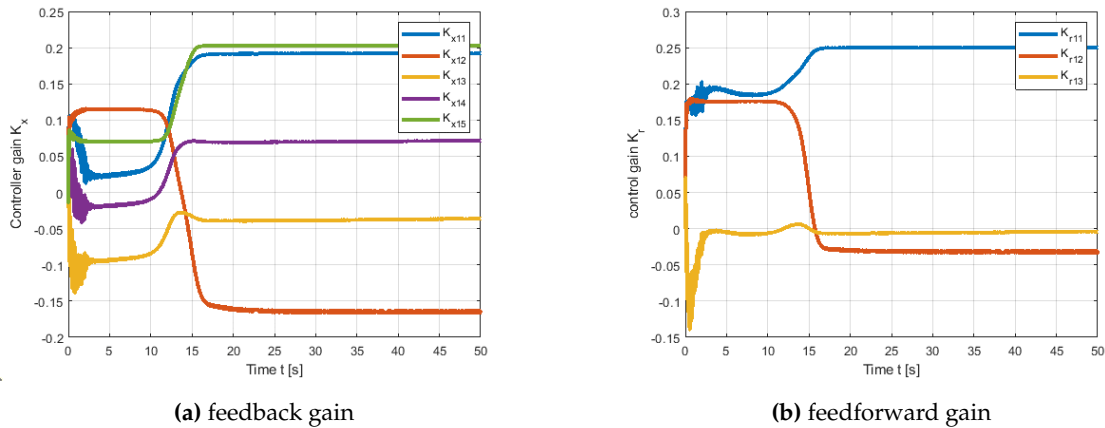


(e) Behavior of yaw angle rate

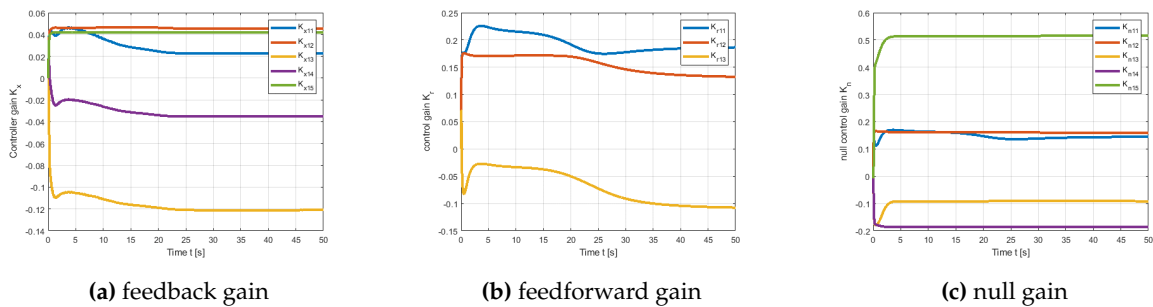
Figure 12. System states with Reference, MRAC, and Modified MRAC.



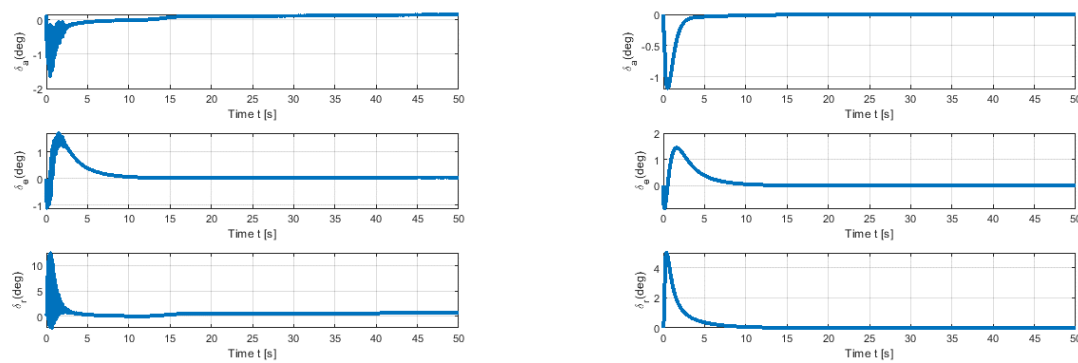
(a) MRAC tracking errors (b) Modified MRAC tracking errors vs.t.
Figure 13. Error dynamics with MRAC and modified MRAC.



(a) feedback gain (b) feedforward gain
Figure 14. MRAC adaptive parameters.



(a) feedback gain (b) feedforward gain (c) null gain
Figure 15. Modified MRAC adaptive parameters.



(a) MRAC control variables

(b) Modified MRAC control variables

Figure 16. MRAC and modified MRAC control commands.

4. Conclusions

This article contributes to existing research in model reference adaptive control theory, by presenting a generalized dynamic inversion and null space parameterization. The adaptive system's closed-loop simulations reveal a highly satisfying performance concerning guaranteed error convergence asymptotically to zero and better transient response. The developed GDI control law is separated into two sections: the first section is referred to as the particular section, and it was used to formulate the reference model trajectories by applying the stipulated dynamic constraints on the system. The other component is the null control vector, which was projected onto the null space of control coefficients and then supplemented into the MRAC control law to enhance performance. The effective implementation of GDI demonstrates that this approach has the potential to simplify adaptive control problems by eliminating the need for complex and tedious procedures. The article's future work will include robustizing the approach versus nonlinear uncertainty and measurement noise, as well as developing a null control vector to account for these non-parametric uncertainties.

Author Contributions: Conceptualization and methodology, A.M.F; software and result discussions, A.M.F; resources, A.M.F; writing and original draft preparation, A.M.F; review and editing, A.H.B; supervision and administration, A.H.B. All authors have read and agreed to the published version of the manuscript.

Funding: This research received no external funding.

Conflicts of Interest: The authors declare no conflict of interest.

References

1. Narendra, K.S.; Annaswamy, A.M. *Stable adaptive systems*; Courier Corporation, 2012.
2. Åström, K.J.; Wittenmark, B. *Adaptive control*; Courier Corporation, 2013.
3. Sastry, S.; Bodson, M. *Adaptive control: stability, convergence and robustness*. Courier Corporation **2011**.
4. Duarte, M.A.; Narendra, K.S. Combined direct and indirect approach to adaptive control. *IEEE Transactions on Automatic Control* **1989**, *34*, 1071–1075.
5. Slotine, J.J.E.; Li, W. Composite adaptive control of robot manipulators. *Automatica* **1989**, *25*, 509–519.
6. Nakanishi, J.; Farrell, J.A.; Schaal, S. Composite adaptive control with locally weighted statistical learning. *Neural Networks* **2005**, *18*, 71–90.
7. Lavretsky, E. Combined/composite model reference adaptive control. *IEEE Transactions on Automatic Control* **2009**, *54*, 2692–2697.
8. Patre, P.M.; MacKunis, W.; Johnson, M.; Dixon, W.E. Composite adaptive control for Euler–Lagrange systems with additive disturbances. *Automatica* **2010**, *46*, 140–147.
9. Boyd, S.; Sastry, S.S. Necessary and sufficient conditions for parameter convergence in adaptive control. *Automatica* **1986**, *22*, 629–639.
10. Loria, A. Explicit convergence rates for MRAC-type systems. *Automatica* **2004**, *40*, 1465–1468.

11. Krstić, M.; Kokotović, P.V.; Kanellakopoulos, I. Transient-performance improvement with a new class of adaptive controllers. *Systems & Control Letters* **1993**, *21*, 451–461.
12. Datta, A.; Ioannou, P.A. Performance analysis and improvement in model reference adaptive control. *IEEE Transactions on Automatic Control* **1994**, *39*, 2370–2387.
13. Sun, J. A modified model reference adaptive control scheme for improved transient performance. *IEEE Transactions on Automatic Control* **1993**, *38*, 1255–1259.
14. Miller, D.E.; Davison, E.J. An adaptive controller which provides an arbitrarily good transient and steady-state response. *IEEE Transactions on Automatic Control* **1991**, *36*, 68–81.
15. Huang, J.T. Sufficient conditions for parameter convergence in linearizable systems. *IEEE Transactions on Automatic Control* **2003**, *48*, 878–880.
16. Cao, C.; Hovakimyan, N. Design and analysis of a novel adaptive control architecture with guaranteed transient performance. *IEEE Transactions on Automatic Control* **2008**, *53*, 586–591.
17. Landau, I. A survey of model reference adaptive techniques—Theory and applications. *Automatica* **1974**, *10*, 353–379.
18. Duarte, M.A.; Narendra, K.S. Combined direct and indirect approach to adaptive control. *IEEE Transactions on Automatic Control* **1989**, *34*, 1071–1075.
19. Slotine, J.J.E.; Li, W. Composite adaptive control of robot manipulators. *Automatica* **1989**, *25*, 509–519.
20. Lavretsky, E. Combined/composite model reference adaptive control. *IEEE Transactions on Automatic Control* **2009**, *54*, 2692–2697.
21. Bechlioulis, C.P.; Rovithakis, G.A. Adaptive control with guaranteed transient and steady state tracking error bounds for strict feedback systems. *Automatica* **2009**, *45*, 532–538.
22. Na, J.; Chen, Q.; Ren, X.; Guo, Y. Adaptive prescribed performance motion control of servo mechanisms with friction compensation. *IEEE Transactions on Industrial Electronics* **2013**, *61*, 486–494.
23. Eugene, L.; Kevin, W.; Howe, D. Robust and adaptive control with aerospace applications, 2013.
24. Annaswamy, A.; Lavretsky, E.; Dydek, Z.; Gibson, T.; Matsutani, M. Recent results in robust adaptive flight control systems. *International Journal of Adaptive Control and Signal Processing* **2013**, *27*, 4–21.
25. Morse, A.S. High-order parameter tuners for the adaptive control of linear and nonlinear systems. In *Systems, models and feedback: Theory and Applications*; Springer, 1992; pp. 339–364.
26. Miller, D.E.; Davison, E.J. An adaptive controller which provides an arbitrarily good transient and steady-state response. *IEEE Transactions on Automatic Control* **1991**, *36*, 68–81.
27. Bajodah, A. Generalised dynamic inversion spacecraft control design methodologies. *IET control theory & applications* **2009**, *3*, 239–251.
28. Bajodah, A. Asymptotic generalised dynamic inversion attitude control. *IET Control Theory & Applications* **2010**, *4*, 827–840.
29. H. Bajodah, A. Asymptotic perturbed feedback linearisation of underactuated Euler’s dynamics. *International Journal of Control* **2009**, *82*, 1856–1869.
30. Bajodah, A.H. Servo-constraint generalized inverse dynamics for robot manipulator control design. 2009 IEEE International Conference on Control and Automation. IEEE, 2009, pp. 1019–1026.
31. Greville, T. The pseudoinverse of a rectangular or singular matrix and its application to the solution of systems of linear equations. *SIAM review* **1959**, *1*, 38–43.
32. Ben-Israel, A.; Greville, T.N. *Generalized inverses: theory and applications*; Vol. 15, Springer Science & Business Media, 2003.
33. Bajodah, A.H.; Hodges, D.H.; Chen, Y.H. Inverse dynamics of servo-constraints based on the generalized inverse. *Nonlinear Dynamics* **2005**, *39*, 179–196.
34. Narendra, K.S.; Annaswamy, A.M. *Stable adaptive systems*; Courier Corporation, 2012.
35. Tao, G. *Adaptive control design and analysis*; Vol. 37, John Wiley & Sons, 2003.
36. Lixin, W.; Zhang, N.; Ting, Y.; Hailiang, L.; Jianghui, Z.; Xiaopeng, J. Three-axis coupled flight control law design for flying wing aircraft using eigenstructure assignment method. *Chinese Journal of Aeronautics* **2020**, *33*, 2510–2526.

Disclaimer/Publisher’s Note: The statements, opinions and data contained in all publications are solely those of the individual author(s) and contributor(s) and not of MDPI and/or the editor(s). MDPI and/or the editor(s) disclaim responsibility for any injury to people or property resulting from any ideas, methods, instructions or products referred to in the content.